J. Am. Chem. Soc. **1989**, *111*, 2409-2417

as the *A*-factor remains constant.

Structures for the various Mn(CO)$_x^+$ ions were assumed as noted. Mn(CO)$_6^+$ was assumed to be an octahedral complex with Mn–C bond lengths of 1.87 Å and C–O bond lengths of 1.14 Å.

Two possibilities are considered for Mn(CO)$_5^+$: a C_{4v} structure resulting from removal of one CO ligand from octahedral Mn(CO)$_6^+$ and a rearranged trigonal-bipyramidal structure. The C_{4v} geometry has been predicted by Burdett for a singlet d^6 metal pentacarbonyl.[14] Further support for the C_{4v} geometry comes from X-ray crystallographic data[50] and gas-phase electron diffraction data[51] for HMn(CO)$_5$, as well as modified extended Hückel calculations[45] on Mn(CO)$_5^+$. Bond lengths were taken from theory.[45] The isoelectronic Cr(CO)$_5^+$ has also been determined to have C_{4v} geometry on the basis of its infrared spectrum.[52] Fe(CO)$_5^+$, on the other hand, is believed to be trigonal bipyramidal.[14]

For Mn(CO)$_4^+$, C_{2v}, D_{4h}, and T_d geometries were considered. It has been predicted that singlet d^6 tetracarbonyls should have the C_{2v} geometry.[14] Infrared spectra[53] and CO addition rates[4,5] for the isoelectronic Cr(CO)$_4$ indicated that this molecule has a C_{2v} ground state, while modified extended Hückel calculations[54] on neutral Mn(CO)$_4$ also predict this structure. Calculated bond lengths were used.[45] Burdett argues, on the basis of theory, that quintet d^6 metal tetracarbonyls should have the T_d structure.[14]

Three geometric possibilities, C_{3v}, D_{3h}, and C_{2v}, are considered for Mn(CO)$_3^+$. Burdett has predicted that the C_{3v} d^6 metal tricarbonyl has a singlet ground state, while the C_{2v} geometry results in a triplet and the D_{3h} geometry is a quintet. Infrared spectral data[53] for the isoelectronic neutrals Mo(CO)$_3$ and Cr(CO)$_3$ are consistent with C_{3v} geometry for both species. Bond lengths were assumed: Mn–C, 1.84 Å; C–O, 1.15 Å.

Appendix B: Method of Calculation

Fits of theoretical kinetic energy release distributions to the measured experimental distributions were obtained as follows. Initially, a guess was made for the bond energy in question, and this value was used to estimate metastable internal energies assuming the low extreme for log *A* as discussed above. Decomposition rate constants were calculated using RRKM theory,[55] with the assumed bond energy and log *A*, for a range of ion internal energies. The internal energies were then assigned weights by using the calculated rate constants in eq 6, and phase space calculations[56] were performed using the weighted internal energies. The same bond energy was used in the phase space calculation as was assumed for the RRKM calculation. On the basis of the comparison of the calculated kinetic energy distribution to the experimental distribution, the bond energy was revised and the process was repeated with a new RRKM calculation. This iteration was continued until the bond energy was bracketed for the low log *A* value, generally to ±0.5 kcal/mol. At that point the high value for log *A* was assumed, a new guess was made for the bond energy, and iterations were performed until the fit converged on a bond energy at the high log *A* value. It is important to note that RRKM theory was used only to determine the metastable internal energies; otherwise, the phase space calculations and fitting procedures did not depend on the RRKM calculations.

---

(50) La Placa, S. J.; Hamilton, W. C.; Ibers, J. A. *Inorg. Chem.* **1964**, *3*, 1491-1495.

(51) Robiette, A. G.; Sheldrick, G. M.; Simpson, R. N. F. *J. Mol. Struct.* **1969**, *4*, 221-231.

(52) Huber, H.; Kundig, E. P.; Ozin, G. A.; Poe, A. J. *J. Am. Chem. Soc.* **1975**, *97*, 308-314.

(53) Perutz, R. N.; Turner, J. J. *J. Am. Chem. Soc.* **1975**, *97*, 4800-4804.

(54) Elian, M.; Hoffmann, R. *Inorg. Chem.* **1975**, *14*, 1058-1076. Also see ref 45.

(55) RRKM calculations were performed using: Hase, W. L.; Bunker, D. L. *A General RRKM Program*. Grouped harmonic frequency direct counting was used to determine sums and densities of states in the activated complexes, while the Whitten-Rabinovitch approximation[35] was used for energized molecules.

(56) A more recent version of the phase space programs used has been submitted to QCPE: Chesnavich, W. J.; Bass, L.; Grice, M. E.; Song, K.; Webb, D. A. TSTPST: Statistical Theory Package for RRKM/QET/TST/PST Calculations *QCPE*, submitted for publication.

Interaction of Triplet Sensitizers with Chlorophyll: Formation of Singlet Chlorophyll[1]

Cornelia Bohne[2] and J. C. Scaiano*

Contribution from the Division of Chemistry, National Research Council of Canada, Ottawa, Ontario, Canada K1A OR6.
Received August 9, 1988

Abstract: The interaction of several triplet sensitizers with chlorophyll *a* (Chl*a*) has been examined using laser techniques. For the carbonyl sensitizers (with triplet energies >53 kcal/mol) it was possible to measure the quenching rate constants; these were systematically $\geq 10^{10}$ M^{-1} s^{-1}. In the cases of acetone, benzophenone, and *p*-methoxyacetophenone the quenching process leads to the formation of the fluorescent singlet state of Chl*a*. For benzophenone ($k_q = 2.4 \times 10^{10}$ M^{-1} s^{-1}) approximately 3% of the quenching events lead to the formation of excited Chl*a*. Several sensitizers (decafluorobenzophenone, benzil, and fluorenone) do not induce Chl*a* fluorescence (or do it very inefficiently) in spite of having triplet energies above the S_1 level of Chl*a*. In light of our results the most probable mechanism involves energy transfer from the triplet sensitizer to an upper triplet state of Chl*a* (^{3}Chl*a***) which can undergo reverse intersystem crossing to the singlet manifold of Chl*a* and thus induce fluorescence. The inefficient sensitizers are those where electron transfer between the excited singlet of Chl*a* or ^{3}Chl*a*** and ground-state sensitizers is energetically favorable, leading to rapid in-cage quenching of the initially formed excited states of Chl*a*. Formation of radical-ion pair between the triplet sensitizer and Chl*a* followed by the generation of singlet Chl*a* in the recombination of the radical ions could not be completely discarded.

Chlorophyll *a* (Chl*a*) fluorescence can be induced by enzymatically generated triplet carbonyl compounds. This process has been observed for Chl*a* in various media, such as aqueous or micellar solutions, when part of chloroplasts or thylakoid fractions, and when bound to serum albumins.[3,4] Two possible mechanisms were suggested: (i) triplet–triplet energy transfer to an upper triplet of Chl*a* and a subsequent population of its S_1 state by reverse intersystem crossing (RISC),[3] or (ii) radical-ion pair formation between the triplet sensitizer and Chl*a* followed by

---

(1) Issued as NRCC-29983.

(2) Postdoctoral Fellow from the Conselho Nacional de Desenvolvimento Cientifico e Tecnologico (CNP$_q$), Brazil.

(3) Bohne, C.; Campa, A.; Cilento, G.; Nassi, L.; Villablanca, M. *Anal. Biochem.* **1986**, *155*, 1.

(4) Bohne, C.; Faljoni-Alario, A.; Cilento, G. *Photochem. Photobiol.* **1988**, *48*, 341.

0002-7863/89/1511-2409$01.50/0 Published 1989 by the American Chemical Society

generation of excited Chl*a* in the radical-ion recombination reaction.[4]

Examples of triplet–singlet energy transfer in which an acceptor is excited through a RISC mechanism are well known in the case of 9,10-dibromoanthracene,[5-10] and it has been proposed for xanthene dyes containing heavy-atom substituents.[11] RISC processes have also been reported in molecules that do not contain heavy atoms; such examples include isoalloxazines[12] and anthracene and its derivatives.[13]

The elucidation of the details of a net triplet–singlet energy transfer mechanism is important, given the spin-forbidden nature of the process. Beside this primary interest, a better understanding of this process could lead to a more accurate definition of the requirements for the detection of triplet species in biological systems using Chl*a* luminescence as a probe. It has been shown that chlorophylls in isolated chloroplasts (from spinach), or when this organelle is part of *Euglena gracillis* (a protozoa), show induced fluorescence and are bleached in the presence of enzymatically generated triplet species.[3,14]

In this paper we report the results of a study of the interaction of triplet sensitizers with Chl*a*, which has been shown to induce Chl*a* fluorescence. In the case of the Chl*a*/benzophenone system we have also been able to estimate the efficiency of the triplet–singlet energy transfer process.

Experimental Section

Materials. Chlorophyll *a* (Chl*a*) from Sigma, acetone (ACS grade from Fisher), acetonitrile (spectroscopic grade from BDH), anthracene from Eastman Kodak, and absolute ethanol (Consolidated Alcohols Ltd.) were used as received. Benzophenone (BP), *p*-methoxyacetophenone (PMAP), *o*-hydroxybenzophenone (OHBP), benzil, fluorenone, and 1,2-benzanthracene from Aldrich were recrystallized from ethanol/water. Decafluorobenzophenone (DFBP) from Aldrich was purified by sublimation.

Stock solutions of all sensitizers were prepared in acetonitrile, and for Chl*a* the stock solutions were in ethanol or acetonitrile–ethanol (8:1). The concentrations of Chl*a* in acetonitrile were determined spectrophotometrically based on extinction coefficients of 6.9×10^4 and 8.5×10^4 M^{-1} cm^{-1} at 662 and 432 nm, respectively.[15]

All experiments were carried out in samples deaerated by nitrogen bubbling for approximately 15 min.

General Techniques. UV-visible absorption spectra were obtained on a HP-8451A diode array spectrometer. Some redox properties were determined by Dr. Fred Hartstock (NRC) using cyclic voltammetry.

Steady-state (prompt) fluorescence spectra were recorded on a Perkin-Elmer LS-5 spectrofluorimeter controlled by a PE-3600 data station. Fluorescence lifetimes were measured on a PRA single photon counting instrument employing a hydrogen lamp for excitation.

Laser Photolysis Experiments. The samples for these experiments were contained in quartz cells constructed of 7×7 mm^2 Suprasil tubing. Static cells typically contained 2.5 mL of solution. For the flow experiments the irradiation cell was built of the same tubing as above and was connected with Teflon tubing to a reservoir where the solutions were deaerated. Flow rates were high enough to ensure reproducible results for Chl*a* emission intensities.

The laser flash photolysis system at NRC and modifications for two-laser experiments have been described earlier.[16,17] A Lumonics TE-860-2 excimer laser operated with Xe/HCl/He mixtures (308 nm, ~5 ns, ≤20 mJ/pulse), a Molectron UV-24 nitrogen laser (337.1 nm, ~8 ns, ≤10 mJ/pulse), or a Candela 500M flash-pumped dye laser (Coumarin 480 or Oxazine perchlorate 720 dyes in 50% aqueous methanol, ~250 ns, 100–350 mJ/pulse) were employed for excitation.

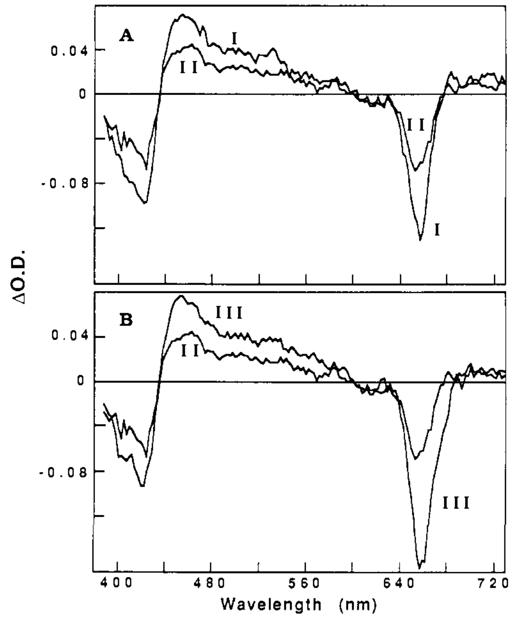

Figure 1. Transient absorption spectra 1.0 μs after the laser pulse (20-ns gate) of triplet Chl*a* alone (I) and in the presence of OHBP (II) or acetone (III). [Chl*a*] = 10 μM, [OHBP] = 0.5 mM, and [acetone] = 0.27 M.

Three types of detection were employed. For time-resolved experiments the signals from an RCA-4840 photomultiplier were captured by either a Tektronix R7912 transient digitizer interfaced to a PDP11/23$^+$ computer, or a Transiac 2001 digitizer interfaced to a PDP11/73 computer via a Camac crate. The latter is better suited for slow kinetics and shares the same optical system as the OMA detector described below. Spectrally resolved data (absorption or emission) were recorded with a Series III gated intensified optical multichannel analyzer (OMA) from EG&G operated by a PDP11/73 computer via an EG&G Model 1461 interface. Detection gates were either 20 ns or a continuously adjustable gate for times in excess of 120 ns. This system has remarkable sensitivity for low levels of emission. The delay between laser excitation and the opening of the OMA gate can be controlled in 10-ns steps. Emission intensities measured with the OMA are relative ones and depend on the alignment of the system. Emission intensity values can only be compared for experiments performed on the same day.

Magnetic fields were applied by a "home-made" magnet which allows continuous variation of the field strength up to 5.4 kG.

Results

Unless otherwise indicated, all the experiments described below were performed at room temperature under oxygen-free conditions, using acetonitrile as solvent.

Transient Absorption Spectra. The characteristic triplet–triplet (TT) absorption spectrum of Chl*a* was produced by direct (308 nm) excitation of a 1.1×10^{-5} M acetonitrile solution of Chl*a*. This spectrum is shown in Figure 1 and agrees well with literature reports.[18] Typical triplet half-lives under our deaerating conditions were ~20 μs.

Chl*a* is not transparent at 308 nm, where our sensitizers are usually excited. Naturally the light absorbed by a given concentration of Chl*a* is less in the presence than in the absence of triplet sensitizers. In order to evaluate quantitatively our data (vide infra), it is necessary to determine the signal intensity which is due to direct excitation of Chl*a*. While a calculated correction based on Beer's law is possible, such a correction does not take into account that the distribution of transients across the reaction cell is a function of the total absorbance at the laser wavelength. In order to achieve matched conditions with our sensitizers (same

---

(5) Kobayashi, S.; Kikuchi, K.; Kokubun, H. *Chem. Phys. Lett.* **1976**, *62*, 494.

(6) Kobayashi, S.; Kikuchi, K.; Kokubun, H. *Chem. Phys.* **1978**, *27*, 399.

(7) Kikuchi, K.; Fukumura, H.; Kokubun, H. *Chem. Phys. Lett.* **1986**, *123*, 226.

(8) Wilson, T.; Halpern, A. M. *J. Am. Chem. Soc.* **1980**, *102*, 7272.

(9) Catalani, L. H.; Wilson, T. *J. Am. Chem. Soc.* **1987**, *109*, 7458.

(10) McGimpsey, W. G.; Scaiano, J. C. *J. Am. Chem. Soc.* **1988**, *110*, 2299.

(11) Duran, N.; Cilento, G. *Photochem. Photobiol.* **1980**, *32*, 113.

(12) Richter, C.; Hub, W.; Traber, R.; Schneider, S. *Photochem. Photobiol.* **1987**, *45*, 671.

(13) Fukumura, H.; Kikuchi, K.; Koike, K.; Hiroshi, K. *J. Photochem. Photobiol. A* **1988**, *42*, 283.

(14) De Mello, M. P.; Nascimento, A.L.T.O.; Bohne, C.; Cilento, G. *Photochem. Photobiol.* **1988**, *47*, 457.

(15) Seely, G. R.; Jensen, R. G. *Spectrochim. Acta* **1965**, *21*, 1835.

(16) Scaiano, J. C. *J. Am. Chem. Soc.* **1980**, *102*, 7747.

(17) Scaiano, J. C.; Tanner, M.; Weir, D. *J. Am. Chem. Soc.* **1985**, *107*, 4396.

(18) Ford, W. E.; Tollin, G. *Photochem. Photobiol.* **1982**, *35*, 809.

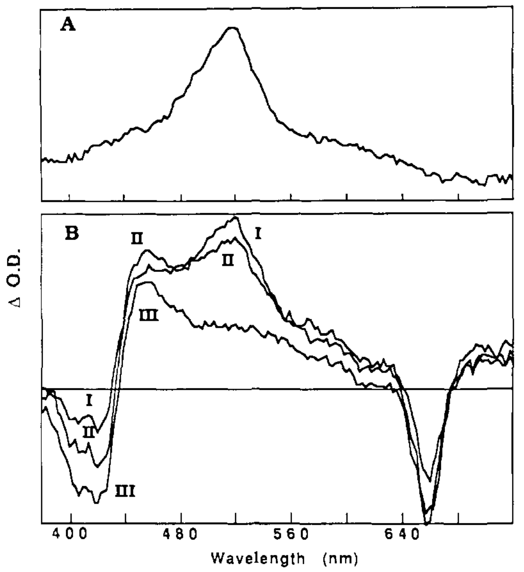

Figure 2. Transient absorption spectra of triplet BP (A) and of the BP/Chl*a* system (B) at 0.2 (I), 1.0 (II, A), and 10 μs (III) after the laser pulse (20-ns gate). [Chl*a*] = 11 μM; [BP] = 10 mM.

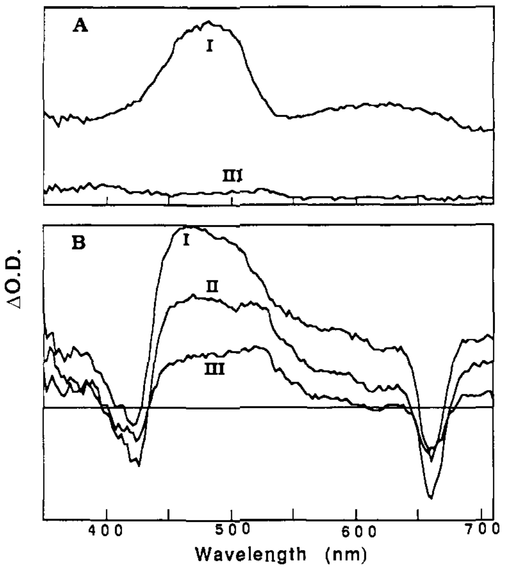

Figure 3. Transient absorption spectra of triplet DFBP(A) and of the DFBP/Chl*a* system (B) at 0.2 (I), 1.0 (II), and 10 μs (III) after the laser pulse (20-ns gate). [Chl*a*] = 11 μM; [DFBP] = 1.1 mM.

absorbance at 308 nm), we have employed *o*-hydroxybenzophenone (OHBP) as a UV screen; the approach is similar to the one employed in singlet oxygen studies reported from this laboratory.[19] OHBP is used as a photochemically inert molecule, taking advantage of the rapid deactivation of its excited state by reversible intramolecular hydrogen transfer; at room temperature OHBP does not yield any detectable signals in the nanosecond time scale, and does not induce any changes in the emission or ground-state absorption spectra of Chl*a*. Figure 1 also shows a Chl*a* TT absorption spectrum obtained in the presence of OHBP. The approach described above allows the evaluation of signals from direct excitation of Chl*a* under conditions that properly reproduce the absorption *and* spatial distribution obtained in the presence of sensitizers.

When acetone is used as a triplet sensitizer (0.8 total absorbance, 0.6 due to acetone), the concentration of Chl*a* triplet formed in the Chl*a*/acetone system is higher than that formed in a matched Chl*a*/OHBP sample (Figure 1). The absorbance signals corresponding to triplet acetone (<400 nm) are too weak to be detectable in the presence of Chl*a* triplets.

When benzophenone (BP) is used as a sensitizer, its triplet state is readily detectable ($\lambda_{max} \sim 520$ nm).[20] Figure 2 shows the evolution of the transient absorption spectra with time; quite clearly the band at ~520 nm decays more rapidly than the Chl*a* signals, and after ~10 μs the spectrum is dominated by that for triplet Chl*a* (cf. Figure 1). Further, in the early stages of the process (compare spectra I and II in Figure 2B), there is a growth of the triplet Chl*a* absorption (in the 450-nm region) concurrent with triplet BP decay.

The results for *p*-methoxyacetophenone (PMAP) and benzil were similar to those for BP, with triplet PMAP and benzil being readily detectable by its triplet absorption at ca. 390[20] and 480 nm,[20] respectively.

Decafluorobenzophenone (DFBP) was also used as a sensitizer, since its triplet energy (~68 kcal/mol) is the same as that for BP, but its redox properties are very different (vide infra).[21] Transient absorption spectroscopy for the Chl*a*/DFBP system (Figure 3) at short delays (0.2 μs) shows the characteristic Chl*a* triplet bands (positive at 465 nm and negative at 420 and 660 nm) and a shoulder at ca. 500 nm due to triplet DFBP. At 420 and 660 nm some absorption due to triplet DFBP tends to offset partially the bleaching signals due to Chl*a*. At long times an absorption at ~520 nm becomes prominent; this signal is neither due to triplet Chl*a* nor to its radical cation. While no further experiments were performed to identify this species, we note that the ketyl radical, $(C_6F_5)_2\dot{C}OH$, absorbs at 520 nm;[21] further, the ground-state spectrum of Chl*a*/DFBP samples shows extensive changes following laser excitation, particularly in the Soret region.

Triplet Quenching by Chlorophyll *a*. The data in the previous section clearly show that in at least the cases of BP, PMAP, acetone, and benzil triplet quenching takes place with concomitant formation of triplet Chl*a*. In this section we report the results of kinetic measurements of the quenching of triplet sensitizers by Chl*a*. Each system presents different problems, and specific techniques had to be employed in each case.

a. Acetone Triplet Quenching. In the presence of increasing concentrations of Chl*a*, the phosphorescence from acetone is too weak to be detectable in time-resolved measurements under our experimental conditions. As already pointed out, absorption signals due to acetone triplet are also too weak to be monitored in the presence of Chl*a* triplet. We have employed 9,10-dibromoanthracene (DBA) as an emission enhancer.[22-25] The energy-transfer process from triplet acetone to DBA and the fluorescence emission from the latter are fast compared with the triplet acetone lifetime, so that the time evolution of the DBA emission provides a measure of the acetone triplet decay. The fluorescence from DBA is quenched by Chl*a*; while this affects the emission intensity, it has no effect on the lifetimes derived from it at each Chl*a* concentration. Thus, the rate constant for triplet acetone quenching by Chl*a* can be obtained by studying the effect of Chl*a* on the decay of DBA fluorescence induced by triplet acetone. These experiments were performed at constant DBA and acetone concentration. To avoid reabsorption effects at relatively high Chl*a* concentrations, the emission from DBA was monitored at 460 nm, rather than at its maximum (~430 nm). The inset in Figure 4 shows two emission decay traces obtained in the absence and presence of Chl*a*. Prompt DBA fluorescence (note the initial spike in Figure 4) which is induced by direct laser excitation is always detectable immediately following the laser pulse. The triplet acetone decay kinetics are of course monitored from the slower component of the trace, the initial points being ignored

---

[19] Scaiano, J. C.; MacEachern, A.; Arnason, J. T.; Morand, P.; Weir, D. *Photochem. Photobiol.* **1987**, *46*, 193.

[20] Carmichael, I.; Hug, G. L. *J. Phys. Chem. Ref. Data* **1986**, *15*, 1.

[21] Boate, D. R.; Johnston, L. J.; Scaiano, J. C. *Can. J. Chem.*, in press.

[22] This is a well-established technique; triplet energy transfer populates the T_2 state of DBA (~74 kcal/mol) which undergoes reverse intersystem crossing to the fluorescent state (S1).[8,9,23,24]

[23] Vassil'ev, R. F. *Nature (London)* **1963**, *200*, 773.

[24] Belyakow, W. A.; Vassil'ev, R. F. *Photochem. Photobiol.* **1970**, *11*, 179.

[25] The experimental conditions were: [acetone] = 0.27 M; [DBA] = 2.7×10^{-5} M, λ measurement = 460 nm.

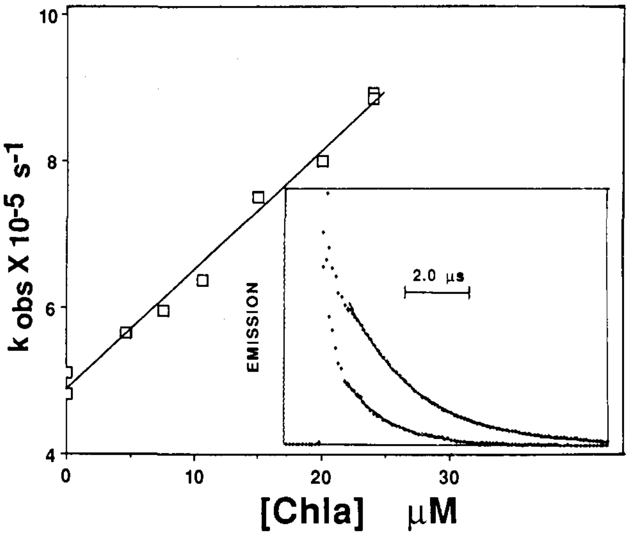

Figure 4. Stern-Volmer plot for the quenching of triplet acetone (0.27 M) by Chl*a*. The acetone decay was monitored at 460 nm using DBA (2.7×10^{-5} M) as an enhancer (see text). The inset shows the decay of acetone/DBA in the absence (slower decay) and presence of 20 µM Chl*a* (faster decay).

Table I. Rate Constants for the Quenching of Different Triplet Sensitizers by Chl*a*

triplet sensitizers	$k_q \times 10^{-10}$, M^{-1} s^{-1}
acetone[a]	1.4 ± 0.2
p-methoxyacetophenone (PMAP)[b]	1.6
benzophenone (BP)[c]	2.4 ± 0.1
decafluorobenzophenone (DFBP)[d]	5.1
benzil[b,c]	4.1 ± 0.7

[a] From DBA-sensitized decay kinetics. [b] From absorption kinetics at 370 nm. [c] From the (I_0/I) vs [Chl*a*] or k_{obs} vs [Chl*a*] (k_{obs} obtained by plotting emission intensities vs. different delay times). [d] From emission kinetics at 460 nm.

for the curve fitting. Figure 4 shows a plot of the rate constant for triplet decay as a function of Chl*a* concentration; from the slope of this plot we obtain a rate constant for triplet quenching, k_q, of $(1.4 \pm 0.2) \times 10^{10}$ M^{-1} s^{-1}.

b. Quenching of Triplet *p*-Methoxyacetophenone. The quenching of triplet PMAP by Chl*a* was monitored following the TT absorption from PMAP at 370 nm.[26] This wavelength corresponds to approximately an isosbestic point between the ground and triplet states of Chl*a*, and therefore the evolution of Chl*a* signals does not interfere with the triplet PMAP decay measurements. The quenching rate constant obtained from the slope of a plot of the rate constant for triplet decay vs. the concentration of Chl*a* has been included in Table I.

c. Quenching of Triplet Benzophenone. The decay of the triplet state of benzophenone could be followed by monitoring the phosphorescence from benzophenone that is readily detectable in the presence of Chl*a*. This is illustrated in the inset in Figure 5, where the short wavelength emission corresponds to benzophenone phosphorescence and the long wavelength band to Chl*a* fluorescence. Measuring the BP phosphorescence was preferred over transient absorption because of the extensive interference by triplet Chl*a* generated by direct excitation (see Figure 2).

When the BP phosphorescence is monitored with a gated OMA detector, the emission intensities in the presence and absence of quencher (I_0/I) depend on the concentration of Chl*a* according to the equation[27]

$$\ln (I_0/I) = k_q t_d [\text{Chl}a] \tag{1}$$

where k_q is the rate constant for triplet quenching and t_d the delay between excitation and the monitoring gate.[28] Figure 5 shows a plot according to eq 1 which leads to $k_q = 2.4 \times 10^{10}$ M^{-1} s^{-1}.

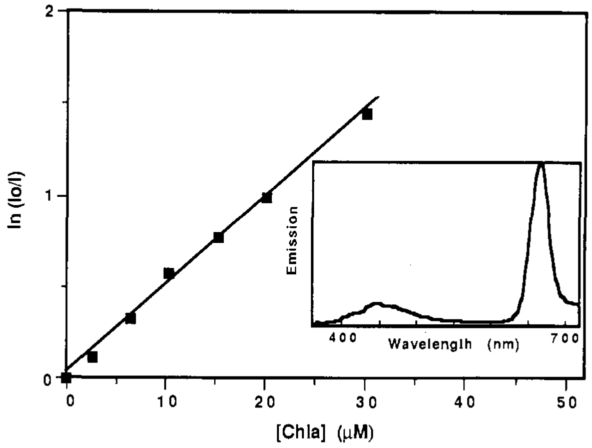

Figure 5. Stern-Volmer plot (gated measurement; see text) for the quenching of triplet BP (10 mM) by Chl*a*. The BP phosphorescence spectra were measured 2.0 µs after the laser pulse with a 20-ns gate. The inset shows the emission spectrum of BP/Chl*a* 1.0 µs after the laser pulse (20-ns gate). [Chl*a*] = 11 µM; [BP] = 10 mM.

In a second approach the lifetimes for triplet BP (τ_T) at different Chl*a* concentrations were estimated from plots of ln (*I*) against t_d (five points at each Chl*a* concentration). A plot of τ_T^{-1} against the Chl*a* concentration led to $k_q = 2.3 \times 10^{10}$ M^{-1} s^{-1}, in excellent agreement with the value obtained from Figure 5.

d. Quenching of Triplet Benzil. The quenching of this sensitizer was measured by the kinetics of its T-T absorption at 370 nm and by monitoring the phosphorescence of benzil in the presence of Chl*a*.[29] Some benzil-delayed fluorescence (λ_{max} = 510 nm), which is due to triplet-triplet annihilation, is detected beside its phosphorescence. For this reason the area below the benzil phosphorescence spectra was integrated only between 500 and 600 nm. Both methods gave similar results, the mean value being shown in Table I.

e. Quenching of Triplet DFBP. This sensitizer interacted with Chl*a* to lead to transient absorptions showing new intermediates in addition to the triplet states of DFBP and Chl*a*.[30] Irradiation also led to significant permanent changes in the ground-state absorption spectrum (vide infra). For this reason quenching experiments were performed in a flow system. The decay of DFBP phosphorescence was monitored at 460 nm from the slow component of the decay (see discussion for triplet acetone quenching). The quenching rate constant has been included in Table I.

Sensitizer-Induced Chlorophyll Fluorescence. The two lasers available in our laboratory for this type of experiment have excitation wavelengths of 308 and 337 nm. Chl*a* absorbs at both wavelengths with similar extinction coefficients, but most of the sensitizers used have a higher extinction coefficient at 308 nm. To obtain a more selective excitation of the sensitizer, the 308-nm wavelength was employed for our experiments. The sensitizer concentration was chosen so as to obtain an optical density of 0.6 at 308 nm (7-mm pathlength), which corresponds to at least three times the absorption for Chl*a* (at 11 µM, the standard concentration used in our experiments). Under these conditions Chl*a* shows intense prompt fluorescence ($\tau \sim 6$ ns; $\Phi_f = 0.25$), but very weak delayed fluorescence.

Benzophenone, PMAP, and acetone all induce Chl*a* fluorescence. The relative fluorescence intensity for Chl*a* induced by triplet sensitization for matched experiments carried out the same day was BP > PMAP > acetone for a 1-µs delay. The Chl*a* emission intensity in the presence of these donors is at least two orders of magnitude stronger than the delayed fluorescence observed for the same Chl*a* concentration. This delayed fluorescence

---

[26] The experimental conditions were: [PMAP] = 5.0 mM.

[27] Scaiano, J. C.; Becknell, A. F.; Small, R. D. *J. Photochem. Photobiol. A* **1988**, *44*, 99.

[28] The experimental conditions were: [BP] = 10 mM; t_d = 2.0 µs.

[29] The experimental conditions were: [benzil] = 10 mM; t_d = 1.0 µs (OMA measurements); λ measurement = 460 nm (decay measurements).

[30] The experimental conditions were: [DFBP] = 1.1 mM; λ measurement = 460 nm.

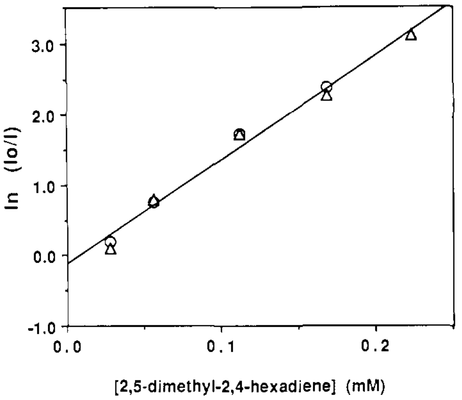

Figure 6. Stern–Volmer plot (gated measurement; see text) for the quenching of BP phosphorescence (○) and Chl*a* induced emission (△) in the BP/Chl*a* system by 2,5-dimethyl-2,4-hexadiene. [BP] = 10 mM; [Chl*a*] = 11 μM; gate = 20 ns; delay = 1 μs.

is due to triplet–triplet annihilation.

In the case of benzophenone, where its phosphorescence and the fluorescence from Chl*a* can be simultaneously monitored (see inset in Figure 5), the intensity ratio between BP phosphorescence and induced Chl*a* fluorescence is the same at different delays between excitation and probing (0.2 to 10 μs range), indicating that both processes are correlated. The fluorescence from Chl*a* in the presence of BP is efficiently quenched by 2,5-dimethyl-2,4-hexadiene, a well-established quencher of BP triplets. Figure 6 shows a Stern–Volmer plot based on both BP phosphorescence and Chl*a* fluorescence; quite clearly the slope is the same for the quenching of both emissions; eq 1 was employed, since the Stern–Volmer expression required is that for gated measurements.

While excitation of BP in the presence of Chl*a* leads to some deterioration of the sample, this process was sufficiently minor that most experiments could be carried out with static samples. This contrasts with the case of acetone, where the fluorescence from Chl*a* decreased with increased number of laser shots, indicating Chl*a* consumption. A luminescence at $\lambda < 450$ nm is observed as the exposure to laser light increased; this emission is probably due to a reaction product. In order to avoid emission from secondary products of reaction, quantitative experiments in which Chl*a* emission intensities were measured had to be performed in a flow system. Under these conditions no significant deterioration of the sample (as judged by Chl*a* emission intensity) results from the experiment, and no emission at $\lambda < 450$ nm can be detected. The phosphorescence from acetone is also too weak to be detectable in the presence of Chl*a* fluorescence.

In order to test whether Chl*a* fluorescence and acetone triplet generation are correlated processes, we measured (1.0 μs after laser excitation) the acetone phosphorescence intensity (integrated between 350 and 480 nm) in the absence of Chl*a* and the Chl*a* fluorescence (integrated between 640 and 700 nm) induced by acetone as a function of laser dose. The Chl*a* fluorescence intensity was monitored in a flow system, as Chl*a* is gradually destroyed in the presence of triplet acetone. The laser dose was adjusted with a calibrated set of neutral density filters. Both of the emissions without neutral density filters were normalized to 100. We have observed a linear relationship (Figure 7) between the intensities of Chl*a* fluorescence and acetone phosphorescence, clearly showing that both processes are correlated.[31] Further, one could hypothesize that Chl*a* fluorescence could result from hetero triplet–triplet annihilation between the triplet sensitizer and triplet Chl*a*, as both are formed by the laser pulse. In such a mechanism, the delayed emission from Chl*a* should follow an approximately quadratic dependence in Figure 7; clearly this is not the case. Similar arguments could be used in the case of BP, where an hetero triplet–triplet annihilation would require that the ratio of the two bands in the inset in Figure 5 be a function of the delay; again, this is not the case. These experiments therefore eliminate hetero triplet–triplet annihilation as a possible origin for the delayed fluorescence observed.

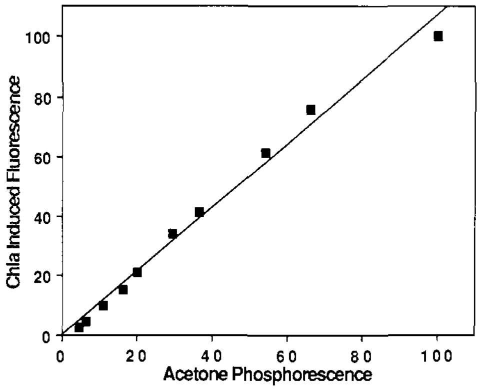

Figure 7. Chl*a* induced fluorescence (by triplet acetone) vs acetone phosphorescence (in the absence of Chl*a*) for different laser doses. [Chl*a*] = 11 μM; [acetone] = 0.27 M.

PMAP is not phosphorescent in solution at room temperature. Excitation of PMAP/Chl*a* samples led to readily detectable Chl*a* delayed fluorescence. Overall the results in this system parallel those already described in the case of BP, except that the ketone phosphorescence is not observable.

A small induced Chl*a* emission is observed in the presence of triplet benzil, which has a triplet energy (54 kcal/mol)[32] higher than the S_1 state of Chl*a* (45.2 kcal/mol).[33] The induced Chl*a* emission intensity is only approximately five times higher at 1.0-μs delay than the intensity due to triplet–triplet annihilation. This was determined in a solution containing added OHBP to match the absorbance at 308 nm to that in the Chl*a*/benzil system. When the contribution from triplet–triplet annihilation is subtracted from the triplet benzil induced emission, the intensity ratios between the Chl*a* emission and benzil phosphorescence are the same at different delays, showing that the processes are correlated.

Triplet fluorenone with an energy similar to benzil (53 kcal/mol)[34] was also used as a sensitizer.[35] The transient absorption spectrum of the fluorenone/Chl*a* system shows the contribution of triplet fluorenone which is evidenced by an apparent decrease of the Chl*a* bleaching at 420 nm and in the 600–700-nm region. The weak Chl*a* emission induced by triplet fluorenone is of the same order of magnitude as that observed in the presence of benzil.

DFBP has almost the same triplet energy (~68 kcal/mol) as BP, but it is more readily reduced than the latter (see below).[21] Chl*a* is not efficiently excited by triplet DFBP, the induced emission also being of the same order of magnitude as the one observed with triplet benzil. After subtracting the emission due to triplet–triplet annihilation, the ratio between the induced Chl*a* emission and DFBP phosphorescence is constant at different delays. Irradiation of the Chl*a*/DFBP system leads to significant changes in the Chl*a* ground-state absorption spectrum, particularly in the Soret region. The changes are different from the bleaching observed with the other sensitizers.

Following a suggestion by one of the reviewers of this paper, we carried out a few experiments to test triplet anthracene and 1,2-benzanthracene[36] as possible sensitizers for Chl*a*. The transient absorption spectra show bands corresponding to the triplet sensitizers and to triplet Chl*a*. In the absence of Chl*a* both sensitizers yield an intense delayed fluorescence in the 400-nm region due to triplet–triplet annihilation. In the presence of Chl*a* the emission of the sensitizer is diminished, while Chl*a* fluorescence (same order of magnitude as in the presence of triplet acetone) is observed.

---

[31] As the acetone phosphorescence is directly proportional to its triplet concentration, this emission intensity was used as a calibration for the triplet concentration at different laser doses.

[32] Murov, S. L. In *Handbook of Photochemistry*; Marcel Dekker: New York, 1973.

[33] Petke, J. D.; Maggiora, G. M.; Shipman, L.; Christoffersen, R. E. *Photochem. Photobiol.* **1979**, *30*, 203.

[34] Yoshihara, K.; Kearns, D. R. *J. Chem. Phys.* **1966**, *45*, 1991.

[35] The standard fluorenone concentration used was 0.5 mM.

[36] The standard anthracene and 1,2-benzanthracene concentrations were 0.5 and 0.3 mM, respectively.

Table II. Thermodynamic and Kinetic Parameters Involving Electron-Transfer Mechanisms

donor	$E_{\mathrm{red}}(\mathrm{S})$,[a] eV	E_{T}, kcal/mol	ΔG_1[b], kcal/mol	ΔG_2[c], kcal/mol	ΔG_3[d], kcal/mol	k_q^s (^{1}Chl*a**) × 10^{-9}, $M^{-1}\,s^{-1}$
acetone	−2.31[e]	80[h]	−14.3	−20.5	+21.1	<0.005
PMAP	−2.28[f]	72[h]	−6.97	−19.8	+20.4	0.03 ± 0.01
BP	−1.84[f]	68[h]	−13.1	−9.68	+10.3	0.20 ± 0.05
DFBP	−1.2[f]	68[i]	−27.9	+5.08	−4.48	2.4 ± 0.3
benzil	−1.17[f]	54[h]	−14.6	+5.77	−5.17	4.2 ± 0.6
fluorenone	−1.33[f]	53[j]	−9.88	+2.08	−1.48	2.1 ± 0.2
1,2-benzanthracene	−2.02[g]	47[g]	+12.0	−13.8		
anthracene	−1.96[g]	42[g]	+15.5	−12.5		

[a] Versus SCE in acetonitrile. [b] ΔG_1, free energy change for radical formation in the interaction of Chl*a* with the triplet sensitizer (Scheme II). [c] ΔG_2, free energy change for radical recombination in which singlet Chl*a* is formed (Scheme II). [d] ΔG_3, free energy change for radical formation in the interaction of the sensitizers with triplet Chl*a* (Scheme III). [e] Reference 42. [f] Reference 43. [g] Reference 44. [h] Reference 32. [i] Reference 21. [j] Reference 34.

In the case of anthracene as a sensitizer the Chl*a* emission induced exceeds the reduction of the intensity of arene delayed emission, while this is not the case for 1,2-benzanthracene.

Efficiency of Chl*a* Excitation in the Chl*a*–Benzophenone System. In this particular system it was possible to estimate the efficiency of singlet Chl*a* excitation resulting from the interaction of triplet BP with Chl*a*. Our measurements are based on a study of the intensity of BP phosphorescence (in the presence of Chl*a*) and of the Chl*a* delayed fluorescence; both were integrated across the emission band. The gate (Δt) selected to collect the emission data was chosen so that it would be longer than the Chl*a* singlet lifetime (τ_f) and shorter than the BP triplet lifetime (τ^0_{BP}), in the absence of Chl*a*. The integrated emission intensities are given by:

$$\int \mathrm{BP} = \alpha_1 k_{\mathrm{ph}}[\mathrm{BP}^*]\Delta t \tag{2}$$

$$\int \mathrm{Chl}a = \alpha_2 \Phi_f k_{\mathrm{ET}}[\mathrm{Chl}a][\mathrm{BP}^*]\Phi_{\mathrm{ex}}\Delta t \tag{3}$$

where α_1 and α_2 are the OMA response factors at the two emission wavelengths ($\alpha_1/\alpha_2 = 3$),[37] k_{ph} is the BP radiative rate constant ($k_{\mathrm{ph}} = 1.2 \times 10^2\ \mathrm{s}^{-1}$),[32] Φ_f is the Chl*a* fluorescence quantum yield in acetonitrile ($\Phi_f = 0.25 \pm 0.03$),[38] k_{ET} is the rate constant for triplet BP quenching by Chl*a* (see Table I), and Φ_{ex} is the efficiency with which energy transfer results in the population of the singlet excited state of Chl*a*. Rearranging the ratio of eq 2 and 3 gives:

$$\int \mathrm{Chl}a = \frac{\alpha_2}{\alpha_1}\frac{\Phi_f k_{\mathrm{ET}}}{k_{\mathrm{ph}}}\Phi_{\mathrm{ex}}\int \mathrm{BP}[\mathrm{Chl}a] \tag{4}$$

In order to avoid interference from Chl*a* reabsorption, the phosphorescence from BP was integrated from 460 to 550 nm, and then corrected to include the complete emission spectrum (300 to 600 nm) by introducing the known emission ratio ∫BP (300–600)/∫BP(460–550) which was independently obtained from a BP phosphorescence spectrum in the absence of Chl*a*. The Chl*a* fluorescence emission was integrated between 600 and 750 nm.

A Φ_{ex} value of 0.03 ± 0.01 was obtained from the slope of the ∫Chl*a* vs. ∫BP(Chl*a*) plot (Figure 8). The linearity of this plot indicates that the measurements performed do not depend on experimental parameters, such as the different gates and delays employed. The error given in the Φ_{ex} value does not include any allowance for errors introduced in Φ_f or k_{ph}.

A second method of obtaining Φ_{ex} was also tested, but found to be subject to many more sources of error than the one described above. Briefly the value of Φ_{ex} can also be obtained from a comparison of the prompt and total delayed fluorescence from Chl*a*. Unfortunately, such an approach relies on the measurement of two emission intensities which are different by several (at least three) orders of magnitude and depends on the lifetime of the BP triplet (frequently not a pure monoexponential); further, it is difficult to account for the laser-induced bleaching of ground-state Chl*a*. Overall this method can be expected to lead to overestimates of Φ_{ex}, and indeed the values obtained systematically exceeded the value of 0.03 given above and were usually several times higher. The value of 0.03 ± 0.01 can, in fact, be regarded as the most reliable estimate.

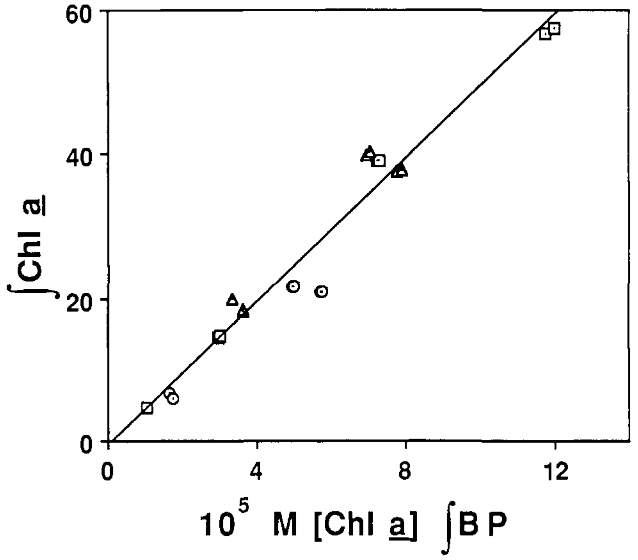

Figure 8. Integrated Chl*a* induced emission (∫Chl*a*) vs integrated BP phosphorescence (∫BP) times the Chl*a* concentration: (□) [Chl*a*] = 3.2 μM, delays 1.0 and 4.0 μs; (○) [Chl*a*] = 6.6 μM, delays 1.0 and 4.0 μs; (△) [Chl*a*] = 8.5 μM, delays 0.5 and 2.0 μs. Two gates (20 and 120 ns) were used for all Chl*a* concentrations.

Singlet Chl*a* Quenching by Ground-State Carbonyl Sensitizers. These studies were performed in aerated solutions,[41] and the Chl*a* fluorescence lifetime ((5.9 ± 0.1)ns) was determined in single photon-counting measurements under identical experimental conditions. All the sensitizers examined quench the Chl*a* fluorescence to some extent, the more efficient ones being DFBP, fluorenone, and benzil. The quenching constants k_q^s are shown in Table II. As the Stern–Volmer constants are rather small, high quencher concentrations had to be added and their stock solutions had to be concentrated (between 0.5 to 2.0 M). This experimental limitation introduces considerable error.

Application of Magnetic Fields. The effect of an external magnetic field (up to 5 kG) on the Chl*a*/BP and Chl*a*/acetone systems was examined. In these experiments we monitored the fluorescence from Chl*a* and the transient absorption at 395 nm; this wavelength was selected because the radical cation from Chl*a*

---

(37) EG&G Technical Catalogue (15439-A-MNL-B, Jan 1986).

(38) The Chl*a* fluorescence quantum yield in acetonitrile was determined by the method of Demas and Crosby[39] assuming $\Phi_f = 0.26$ for Chl*a* in acetone at zero concentration.[40]

(39) Demas, J. N.; Crosby, G. A. *J. Phys. Chem.* **1971**, *75*, 991.

(40) Forster, L. S.; Livingston, R. *J. Chem. Phys.* **1952**, *20*, 1315.

(41) For all sensitizers [Chl*a*] = 2.0 μM. Chl*a* was excited at 418 nm and the emission spectra was integrated between 640 and 700 nm for acetone, PMAP, BP, and DFBP, while for benzil and fluorenone the Chl*a* was excited at 600 nm and the emission spectra were integrated between 650 and 700 nm.

(42) Yip, R. W.; Loufty, R. O.; Chow, Y. L.; Magdzinski, L. K. *Can. J. Chem.* **1972**, *50*, 3426.

(43) Measured by Dr. Fred Hartstock (Division of Chemistry, National Research Council, Ottawa) by cyclic voltammetry.

(44) Weller, A.; Zachariasse, K. *Chem. Phys. Lett.* **1971**, *10*, 197.

Scheme I

$$^3S^* + \mathrm{Chla} \xrightarrow{k_{ET}} S + {}^3\mathrm{Chla}^{**}$$

$$^3\mathrm{Chla}^{**} \longrightarrow {}^3\mathrm{Chla}^*$$

$$^3\mathrm{Chla}^{**} \xrightarrow{\mathrm{RISC}} {}^1\mathrm{Chla}^*$$

is known to absorb strongly.[18] Magnetic fields can be expected to slow down the rate of intersystem crossing in the geminate radical-ion pair (vide infra). Such an effect would lead to a reduced Chl*a* delayed emission and possibly to an enhancement of the absorption at 395 nm. No difference in either was observed upon application of a 5-kG field.

Attempted Two-Laser Two-Color Experiment. These measurements were performed in an attempt to evaluate if reverse intersystem crossing (RISC), i.e., $T_n \rightarrow S_1$, played a role in determining the efficiency of Chl*a* delayed emission reported in this work. Chl*a* triplets were generated by 337-nm laser excitation of Chl*a* (in the absence of sensitizers). The triplet was then excited at either 480 or 720 nm with a broadband flash pumped dye laser. Unfortunately, triplet Chl*a* cannot be selectively excited at these wavelengths, its ground state competing with the triplet for the exciting light. Prompt fluorescence induced by the dye laser is such that it prevented the detection of any RISC-induced emission. Indeed, if the value of 0.03 for Φ_{ex} measured above represented the quantum yield for RISC, it would be too low to be measurable in the presence of prompt emission induced by dye laser excitation of Chl*a* ground state.

Discussion

The delayed Chl*a* fluorescence induced by sensitizer excitation cannot be attributed to singlet sensitization. Even in cases where Φ_{ISC} for the donor is less than one (e.g., acetone), singlet sensitization would occur in a short (a few nanoseconds) time scale rather than the much longer times in which Chl*a* emission was observed. In the case of benzophenone, singlet sensitization would be impossible, since $\Phi_{ISC} = 1.0$ and the singlet lifetime is in the neighborhood of 10 ps.[45]

In the case of anthracene and 1,2-benzanthracene Chl*a* could be excited to some extent through the trivial (emission–reabsorption) mechanism as the delayed emission of these sensitizers is in the region of Chl*a* ground-state absorption. A quantitative differentiation between the trivial and energy-transfer mechanism is not possible, although the more intense Chl*a* emission than the decrease of the anthracene delayed fluorescence suggests that part of the Chl*a* emission is induced by the interaction with the triplet sensitizer.

The excellent match observed between the triplet lifetimes and the delayed fluorescence lifetimes (vide supra) clearly points to the triplet state of the carbonyl sensitizers as the species responsible for sensitization. It is also clear that the emission from Chl*a* in the interaction with carbonyl compounds is not the result of a trivial mechanism involving donor emission and reabsorption by Chl*a*, since the process has been observed with nonphosphorescent donors such as PMAP. In other examples, such as acetone, the emission from Chl*a* is considerably more intense than the donor phosphorescence. The long-range Förster mechanism (dipole–dipole) can also be ruled out. The delayed emission intensities induced by PMAP and acetone triplets are of the same order of magnitude, while the radiative rate constant for PMAP is smaller by a factor of ~20 than for acetone.[32]

From a phenomenological point of view it is clear that quenching of some triplet donors by Chl*a* results in the formation of singlet excited Chl*a* with significant efficiency. With this firmly established, we turn to the question of the mechanism that can lead to this result. Two possible mechanisms have been proposed: (1) energy transfer to an upper triplet state of Chl*a* and subsequent population of S_1 by a RISC process;[3] (2) electron transfer to produce a geminate radical-ion pair, followed by generation of the S_1 state of Chl*a* in the recombination (possibly geminate) of the radical-ion pair.[4] Schemes I and II illustrate the two mechanisms proposed. In these schemes the numeric superscripts indicate multiplicity, the square brackets indicate geminate character, a single asterisk represents the lowest excited state for a given multiplicity, and a double asterisk indicates an upper excited state.

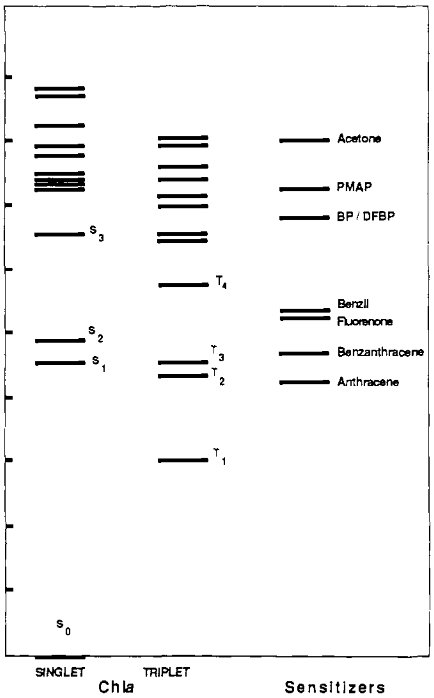

Figure 9. Chl*a* state diagram as calculated by Petke et al.[33] and the triplet energy levels of ail sensitizers used.

Scheme II

$$^3S^* + \mathrm{Chla} \longrightarrow {}^3[S^{\dot{-}} \cdots \mathrm{Chla}^{\dot{+}}] \qquad (\Delta G_1)$$

$$^3[S^{\dot{-}} \cdots \mathrm{Chla}^{\dot{+}}] \longrightarrow S + {}^3\mathrm{Chla}^*$$

$$^3[S^{\dot{-}} \cdots \mathrm{Chla}^{\dot{+}}] \longrightarrow S^{\dot{-}} + \mathrm{Chla}^{\dot{+}}$$

$$^3[S^{\dot{-}} \cdots \mathrm{Chla}^{\dot{+}}] \underset{}{\overset{\mathrm{ISC}}{\rightleftharpoons}} {}^1[S^{\dot{-}} \cdots \mathrm{Chla}^{\dot{+}}]$$

$$^1[S^{\dot{-}} \cdots \mathrm{Chla}^{\dot{+}}] \longrightarrow S + \mathrm{Chla}$$

$$^1[S^{\dot{-}} \cdots \mathrm{Chla}^{\dot{+}}] \longrightarrow S + {}^1\mathrm{Chla}^* \qquad (\Delta G_2)$$

$$^1[S^{\dot{-}} \cdots \mathrm{Chla}^{\dot{+}}] \longrightarrow S^{\dot{-}} + \mathrm{Chla}^{*+}$$

In the mechanism of Scheme I we would expect RISC to be favored for approximately degenerate T_n and S_1 levels and for relatively large T_n–T_{n-1} energy gaps. Small energy gaps within the triplet manifold will tend to lead to efficient internal conversion. Figure 9 shows an energy level diagram for chlorophyll based on studies by Petke et al.[33] We have included in the same diagram the energy levels for the various sensitizers used. The ordering of Chl*a* levels in Figure 9 is believed to be reliable, except perhaps in cases of near degeneracy.[33,46] The RISC requirements mentioned above are most closely met for the T_3/T_2 levels which are

---

(45) Turro, N. J. In *Modern Molecular Photochemistry* **1978**, 179.

(46) Petke et al.[33] stated that the replacement of the phytyl chain of Chl*a* by ethyl does not alter its absorption spectra and so their calculated state diagram for ethyl chlorophyllide *a* is also valid for Chl*a*. The energy levels were determined by ab initio configuration interaction calculations.

Scheme III

$$^3S^* + \mathrm{Chla} \longrightarrow [S + {}^3\mathrm{Chla}^{**}]$$

$$[S + {}^3\mathrm{Chla}^{**}] \longrightarrow [S + {}^3\mathrm{Chla}^{*}] \longrightarrow \text{separation}$$

$$[S + {}^3\mathrm{Chla}^{**}] \longrightarrow {}^3[S^{\cdot-} \cdots\cdots \mathrm{Chla}^{\cdot+}] \qquad (\Delta G_3)$$

$$[S + {}^3\mathrm{Chla}^{**}] \xrightarrow{\text{RISC}} [S + {}^1\mathrm{Chla}^{*}]$$

$$[S + {}^1\mathrm{Chla}^{*}] \longrightarrow {}^1[S^{\cdot-} \cdots\cdots \mathrm{Chla}^{\cdot+}] \qquad (-\Delta G_2)$$

$$[S + {}^1\mathrm{Chla}^{*}] \longrightarrow S + {}^1\mathrm{Chla}^{*}$$

almost degenerate with S_1. The energy gap between T_3/T_2 and T_1 is also relatively large.

The free energy changes for radical pair formation (ΔG_1) and Chl*a* excitation upon recombination (ΔG_2) can be calculated using the same formulas described by Weller for quenching processes involving electron transfer,[47] i.e.

$$\Delta G_1 = 23.06[E_{\mathrm{ox}}(\mathrm{Chl}a) - E_{\mathrm{red}}(\mathrm{S})] - E_{\mathrm{T}} - e^2/\epsilon a \qquad (5)$$

$$\Delta G_2 = E_{\mathrm{S}} + 23.06[E_{\mathrm{red}}(\mathrm{S}) - E_{\mathrm{ox}}(\mathrm{Chl}a)] + e^2/\epsilon a \qquad (6)$$

where $E_{\mathrm{ox}}(\mathrm{Chl}a)$ is the oxidation potential for Chl*a* (0.54 eV vs. SCE in acetonitrile),[48] $E_{\mathrm{red}}(\mathrm{S})$ and E_{T} are the reduction potentials and triplet energies for the sensitizers (see Table II), E_{S} is the singlet energy for Chl*a* (45.2 kcal/mol),[33] and $e^2/\epsilon a$ is the Coulombic term; this last term is small (1.1 kcal/mol when assuming a = 8 Å) and was disregarded in the calculations. The values of ΔG_1 and ΔG_2 for the various donors have been listed in Table II.

The rate constants for quenching of the triplet sensitizers by Chl*a* (Table I) seem to reflect straightforward diffusional quenching. The somewhat higher than diffusion-controlled values for benzil and DFBP (which could reflect the accumulation of products with potentially more efficient quenching rates) would not change the validity of the conclusions presented herein. These values are not so much higher than the diffusion-controlled limit to indicate the participation of other processes such as ground-state complexation. Actually no evidence (UV–vis spectroscopy) for ground-state complexation was obtained.

For all carbonyl sensitizers energy and electron-transfer processes are exothermic (Table II). Both processes probably compete in the Chl*a*–triplet sensitizer encounter complex. Unfortunately, the results with anthracene and 1,2-benzanthracene, for which the electron transfer is endothermic (Table II), are not conclusive as a result of complications derived from their intense delayed fluorescence.

The results presented cannot be fully explained by the mechanisms outlined in Schemes I and II. The excitation of Chl*a* is dependent on the reduction potential of the sensitizers as all their triplet energies are high enough to excite the upper triplet states of Chl*a*. On the other hand, if the electron-transfer mechanism was operative, the lack of detection of the Chl*a* cation radical could only be explained by a much faster back-electron-transfer process than radical separation. In this case the limiting step in Scheme II would be the intersystem crossing in the geminate radical ion pair and a magnetic field effect on the Chl*a* luminescence should have been observed.

A mechanism which takes into account the energy *and* redox properties of the sensitizer is shown in Scheme III. The brackets mean that the processes after energy-transfer occur in the solvent cage. In this mechanism the redox properties of the sensitizer play a role in the fate of the excited Chl*a* in quenching the upper triplet state (T_3/T_2) and/or singlet Chl*a* by a charge or electron-transfer mechanism. The values of ΔG_3 have also been included in Table II and are based on a triplet energy of 44.6 kcal/mol (average of calculated T_2 and T_3).[33] The similarity between ΔG_3 and $-\Delta G_2$ is a reflection of the fact that S_1 and T_2/T_3 are almost degenerate. The $-\Delta G_2$ and ΔG_3 values show that DFBP, benzil, and fluorenone could quench Chl*a*, explaining why with these sensitizers no Chl*a* emission is observed.

The quenching of singlet Chl*a* by the ground-state carbonyl sensitizers (Table II, $k_q{}^s$) is in agreement with the mechanism in Scheme III as the quenching constants correlate with the reduction potentials of the sensitizers. Probably a electron- or charge-transfer mechanism is operative. Given that S_1 and T_2/T_3 are almost degenerate and that the redox properties of excited Chl*a* are not expected to change significantly as a result of the different multiplicities, quenching of the upper triplet Chl*a* by the sensitizers is also expected.

Excited singlet Chl*a* is quenched by nitroaromatic compounds through a charge-transfer mechanism, the quenching rate constants correlating with the reduction potentials of these acceptors.[49] For weakly oxidizing nitroaromatic acceptors covalent exciplexes with Chl*a* were proposed, whereas the exciplex for strongly oxidizing acceptors should have a considerable ionic character. The quenching rate constant of singlet Chl*a* by DFBP, benzil, and fluorenone are in agreement with the value for nitrobenzene[49] derivatives with similar reduction potentials. If in our system a geminate radical-ion pair was formed as a result of singlet Chl*a* quenching by ground-state sensitizers, the back-electron-transfer reaction would have to be efficient for the sensitizers with high ^{1}Chl*a** quenching rate where quenching would be competitive with cage escape. This would explain why in our systems no radicals were detected. The competition between back-electron-transfer and cage escape was described for other systems.[50]

As shown in Scheme III the generation of ^{3}Chl*a*** and/or ^{1}Chl*a** always occurs in the solvent cage, where the sensitizer is still present. For sensitizers that do not induce Chl*a* emissions, the quenching of ^{3}Chl*a*** and/or ^{1}Chl*a** is exothermic (ΔG_3 and $-\Delta G_2 < 0$). Although the quenching rate constant for singlet Chl*a* is not diffusion controlled, it may only represent a lower limit for the process occurring in the solvent cage, as specific orientations achieved during the preceding energy transfer ($^3S^* \rightarrow {}^3\mathrm{Chl}a^{**}$) could facilitate the quenching of excited Chl*a*. For the sensitizers that induce Chl*a* emission, their singlet Chl*a* quenching rate is at least one order of magnitude smaller, and thus excited Chl*a* should readily escape from the solvent cage.

From the Φ_{ex} value of 0.03 measured for Chl*a* in the presence of triplet BP, it is possible to estimate the lifetime of the T_2/T_3 state if one assumes that RISC involves the same states as S → T intersystem crossing. On this assumption, and taking τ_{S} = 6 ns, Φ_{ISC} = 0.75, and $k_{\mathrm{ISC}} = 1.3 \times 10^8$ s^{-1}, one can calculate a lifetime of 0.2–0.5 ns. This appears too long considering that the energy difference between T_3/T_2 and T_1 is around 15 kcal/mol and internal conversion should be fast. A likely explanation for this apparent discrepancy is that if the energy of T_3/T_2 is slightly higher than S_1, than RISC may involve a set of states (i.e., $T_3/T_2 \rightarrow S_1$) different from normal intersystem crossing (probably $S_1 \rightarrow T_1$); if this is the case, the estimation above would not be valid and a much shorter lifetime for T_3/T_2 would be fully consistent with the data. The only requirement for this would be an error of ca. 2 kcal/mol in the calculated energy level for T_3/T_2.

The pure electron-transfer mechanism (Scheme II) above was discarded because of the lack of a magnetic field effect and the lack of detection of the Chl*a* cation radical. We are aware that these negative observations may not be conclusive, but although we cannot fully differentiate between these two mechanisms, the

---

(47) Rehm, D.; Weller, A. *Isr. J. Chem.* **1970**, *8*, 259.

(48) Seely, G. R. *Photochem. Photobiol.* **1978**, *27*, 639.

(49) Droupadi, P. R.; Krishman, V. *Biochim. Biophys. Acta* **1987**, *894*, 284.

(50) Gould, I. R.; Ese, D.; Mattes, S. L.; Farid, S. J. *J. Am. Chem. Soc.* **1987**, *109*, 3794.

one in Scheme III is in better agreement with the results presented.

In conclusion, it was shown that the redox properties of a triplet sensitizer are crucial to Chl*a* singlet state formation. The excitation yield of 0.03 measured in the benzophenone/Chl*a* system indicates a rather efficient process when one takes into account the spin-forbidden nature of the process and the absence of heavy atoms.

The fact that in the excitation of Chl*a* to its singlet state by a triplet sensitizer the redox properties of the latter are important has to be considered when this molecule is used to detect enzymatically generated triplet species. In the case of the operation of the mechanism outlined in Scheme III, the charge or electron-transfer of an acceptor primarily excited by a triplet molecule could be important in the interaction of enzymatically generated triplet species with biomolecules, where processes could be triggered in which an energy transfer would be coupled to electron transfer.

Acknowledgments. Thanks are due to Dr. F. Hartstock for the measurement of the reduction potentials of the different sensitizers, to Mr. S. E. Sugamori for technical assistance, and to Dr. L. J. Johnston for her help in the early stages of this work.

SF_6-Sensitized Infrared Photodecomposition of $Fe(CO)_5$

Tetsuro Majima,* Tadahiro Ishii,[†] Yoshiyasu Matsumoto, and Michio Takami

Contribution from the Institute of Physical and Chemical Research, Hirosawa, Wako, Saitama, 351-01, Japan.

Received August 18, 1988

Abstract: The SF_6-sensitized infrared photodecomposition of $Fe(CO)_5$ induced by a transversely excited atmospheric (TEA) CO_2 laser has been studied. The decomposition of $Fe(CO)_5$ proceeds via sequential decarbonylation after thermal equilibrium is attained through collisional V–V and V–T/R processes. $Fe(CO)_4(PF_3)$ is formed as a dominant product at lower conversion in a mixture of SF_6–$Fe(CO)_5$–PF_3, which indicates that the rate-determining process is the first decarbonylation of excited $Fe(CO)_5$ into $Fe(CO)_4$ and CO, and that $Fe(CO)_4$ is trapped by PF_3 to yield $Fe(CO)_4(PF_3)$. In addition, $Fe(CO)_3(PF_3)_2$, $Fe(CO)_2(PF_3)_3$, and $Fe(CO)(PF_3)_4$ are formed progressively with increasing conversion of $Fe(CO)_5$. These higher PF_3-substituted iron complexes are formed by repeated series of thermal excitation, decarbonylation, and trapping by PF_3. Final products are CO and iron particles, following the shot by shot stoichiometry of $Fe(CO)_5 \rightarrow Fe + 5CO$. The iron particles are found to be γ-iron or austenite, (Fe–C)4F, including 0.75 wt % carbon which has a mean particle size of 80 Å and a face-centered-cubic structure. Variations of the decomposition probability by changing the irradiation parameters are qualitatively explained by changes of kinetic temperature in irradiated volume. The decomposition mechanism in SF_6-sensitized infrared photolysis is compared with those in conventional pyrolysis, infrared multiple-photon decomposition, and UV photolysis.

The photochemistry of transition metal carbonyls continues to be of major interest because of the photocatalytic properties of metal carbonyls. Unsubstituted transition metal carbonyls decompose into coordinatively unsaturated species and carbon monoxide(s) by UV and visible light excitation to electronically excited states. Recently much attention has been focused on the coordinatively unsaturated species in solution[1-4] and also in the gas phase[5-7] because of their catalytic activities. In addition to many photochemical studies of metal carbonyls in the visible and UV region, infrared multiple-photon decomposition (IRMPD) of metal carbonyls such as $Ni(CO)_4$, $Fe(CO)_5$, $Cr(CO)_6$, $Mo(CO)_6$, and $W(CO)_6$ has been studied using a frequency-doubled, transversely excited atmospheric (TEA) CO_2 laser at 5 μm[8] and a p-H_2 Raman laser at 16–17 μm.[9] A TEA CO_2 laser as well as a CW CO_2 laser has also been used to decompose metal carbonyls by IR photosensitized reaction[10-12] and by dielectric breakdown.[13]

Since most of the unsubstituted transition metal carbonyls do not absorb or absorb only weakly in the tunable range of a TEA CO_2 laser, it is necessary to add an infrared photosensitizer. Ideally this should be a substance which absorbs the infrared radiation strongly and transfers a sufficient portion of the absorbed energy to the metal carbonyls for decomposition but does not decompose itself or participate in the reaction sequence. It has been well characterized that SF_6 absorbs strongly in the tunable range of a TEA CO_2 laser but does not decompose at a low laser fluence (ca. 2 J cm^{-2}) because of the relatively high threshold fluence for IRMPD.[14-16] The S–F stretching mode (ν_3) of SF_6, centered at 947 cm^{-1},[17] has an exceptionally high extinction coefficient of 0.2 Torr^{-1} cm^{-1} (5.65×10^{-18} cm^2). In fact, SF_6 has been found to be an excellent infrared photosensitizer for inducing decomposition of $Fe(CO)_5$ with a TEA CO_2 laser in a mixture of SF_6, $Fe(CO)_5$, temperature-monitoring gas, and buffer gas with ca. 100 Torr of total pressure.[11,12]

In the present work we studied the infrared photosensitized decomposition of $Fe(CO)_5$ with an interest in using a TEA CO_2 laser for the generation of coordinatively unsaturated species of metal carbonyls as a catalyst. For such application, it should be clarified how activated $Fe(CO)_5$ decomposes into final products,

---

[†] Research Associate from Science University of Tokyo, Kagurazaka, Tokyo 162, Japan.

(1) Geoffroy, G. L.; Wrighton, M. S. *Organometallic Photochemistry*; Academic Press: New York, 1979.

(2) Wrighton, M. S.; Grinley, D. S.; Schroeder, M. A.; Morse, D. L. *Pure Appl. Chem.* **1975**, *41*, 671.

(3) Wrighton, M. S.; Graff, J. L.; Kazlansleas, R. J.; Mitchener, J. C.; Reichel, C. L. *Pure Appl. Chem.* **1982**, *54*, 161.

(4) Whetten, R. L.; Grant, E. R. *J. Am. Chem. Soc.* **1982**, *104*, 4270.

(5) Tumas, W.; Gitlin, B.; Rosan, A. M.; Yardley, J. T. *J. Am. Chem. Soc.* **1982**, *104*, 55.

(6) Whetten, R. L.; Fu, K.-J.; Grant, E. R. *J. Chem. Phys.* **1982**, *77*, 3769.

(7) Miller, M. E.; Grant, E. R. *J. Am. Chem. Soc.* **1984**, *106*, 4635.

(8) Au, M.-K.; Hackett, P. A.; Humphries, M.; John, P. *Appl. Phys. Lett.* **1984**, *B33*, 43.

(9) Majima, T.; Tashiro, H.; Midorikawa, K.; Takami, M. *Chem. Phys. Lett.* **1985**, *121*, 65.

(10) Bristow, N. J.; Moore, B. D.; Poliakoff, M.; Ryott, G. J.; Turner, J. J. *J. Organomet. Chem.* **1984**, *260*, 181.

(11) Smith, G. P.; Laine, R. M. *J. Phys. Chem.* **1981**, *85*, 1620.

(12) Lewis, K. E.; Golden, D. M.; Smith, G. P. *J. Am. Chem. Soc.* **1984**, *106*, 3905.

(13) Langsam, Y.; Ronn, A. M. *Chem. Phys.* **1981**, *54*, 277.

(14) Ambartsumyan, R. V.; Gorohkov, Y. A.; Letohkov, V. S.; Makarov, G. N. *Sov. Phys. JETP* **1975**, *42*, 993.

(15) Lyman, J. L.; Jensen, R. J.; Rinck, J.; Robinson, C. P.; Lockwood, D. *Appl. Phys. Lett.* **1975**, *27*, 87.

(16) Fuss, W.; Cotter, T. P. *Appl. Phys.* **1977**, *12*, 265.

(17) Burak, L.; Houston, P.; Sutton, D. G.; Steinfeld, J. I. *J. Chem. Phys.* **1970**, *53*, 3632.